Current profile modelling in JET and JT-60U identity experiments

P. Sirén[1], T. Tala[1], G. Corrigan[2], J. Garcia[3], X. Litaudon[3], A. Salmi[1], JET EFDA contributors* and the EU-ITM ITER Scenario Modelling Group

JET-EFDA Culham Science Centre, OX15 3DB, Abingdon, UK
[1] Association Euratom-Tekes, VTT, PO Box 1000, 02044 VTT, Finland
[2]CCFE, Euratom Association, Culham Science Centre, Abingdon OX14 3DB, UK
[3]CEA, IRFM, F -13108 St-Paul-Lez-Durance, France
[*]See Romanelli F 2012 Proc. 24nd IAEA Conf. on Fusion Energy 2012 San Diego USA

1. INTRODUCTION

The advanced tokamak (AT) scenario (defined by high fusion efficiency with operation close to steady-state conditions [1]) is one of the most promising ways to achieve the steady-state operation in the forthcoming fusion power plants.

The motivation in AT identity plasma experiments was to study the forming of ITBs and steady-state properties. The experiments in JET and JT-60U in 2008, described (technical details and fulfilling the main goals) in publications [2, 3], were the first experiments where the global plasma parameters and profiles were matched between two similar-size tokamaks with reverse q and the goal of the high bootstrap fraction. The main goal of this paper is to understand the most significant differences between two approximately same-size tokamaks, JET and JT-60U, and study the time evolution of the plasma current density and q by predictive current diffusion simulations.

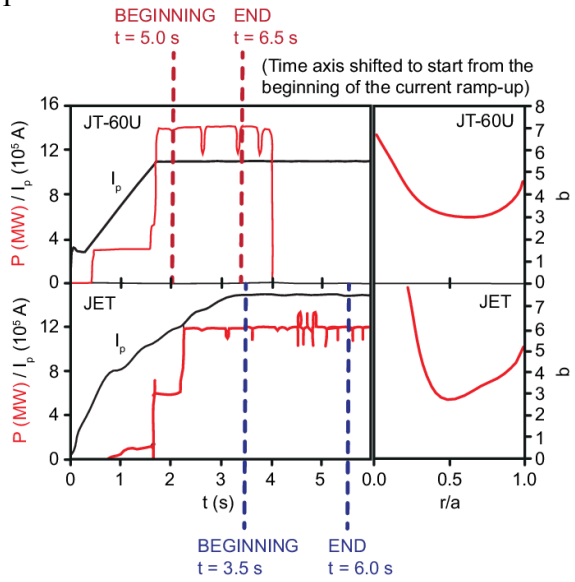

Figure 1: The time window (red: total NBI power, black: plasma current) and the initial q of the discharges JT-60U #49469 (top) JET #74740 (bottom). Time axis has been shifted such that the starting point at t = 0s is the start of the current ramp up.

2. DATA AND MODELLING TOOLS

The experimental data profiles from discharges JET #74740 and JT-60U #49469 (Figure 1) have been used in the simulations (T_e and n_e from Thomson scattering diagnostic, T_i and Z_{eff} from charge exchange spectroscopy, initial q from magnetic data and MSE). The 1.5-dimensional JETTO transport code [4] was used in the predictive current diffusion modelling. Neoclassical effects were calculated by NCLASS [5], NBI current density by ASCOT [6] and plasma equilibrium by ESCO code. The used JETTO simulation model was successfully validated against the experimental data (magnetic+MSE) from both JET and JT-60U (presented in Figure 2).

3. EXPERIMENTAL DATA ANALYSIS

The most significant differences between the shots of JET and JT-60U are the density gradient and the shape of the q-profile which were observed later in the flat top phase. The density gradient is presented in Figure 3.I.a, where it can be seen that a transport barrier is not

observed in the density profile time evolution in JET. Instead, the shot #49469 in JT-60U has a rather strong density gradient at ρ = 0.15-0.50, which produces a considerable peak in the bootstrap current density [7] profile. The bootstrap fraction in JET is less than 30%, whereas in JT-60U the fraction is even 90 % and as high as 40 % also in the later phase. These are significant contributions in the total non-inductive plasma current.

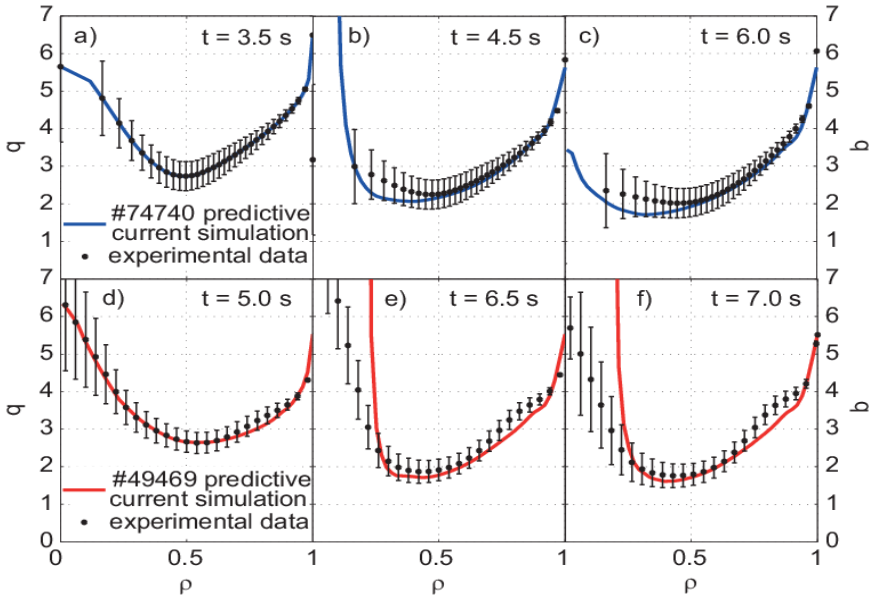

Figure 2: Validation of the JETTO current diffusion model. a-c) Validation with the data from JET #74740 (blue line: JETTO simulation, black markers: magnetic-MSE data). d-f) Validation with the data from JT-60U #49469 (red line: JETTO simulation, black markers: magnetic-MSE data).

4. PREDICTIVE CURRENT DIFFUSION SIMULATIONS

Studying the impact of different NBI-current density profiles has been performed with the simulation cases, where NBI current density in JET was replaced with the corresponding profile from JT-60U and vice versa in JT-60U. The results state that the shape of the NBI current density profile was not a significant factor in controlling the current-density time evolution. Maximum differences with the reference case are 10% (at ρ = 0.25-0.40) which are smaller than the estimated errors in the experimentally determined q. The differences between NBI current density profiles were sufficiently large at ρ < 0.5, but the NBI-current fractions (JET 22%, JT-60U 24%) were approximately the same. Simulations with larger differences, for instance different NBI current fractions, were performed, but this way does not give answers for the different time evolution of the q-profile in these identity experiments and it requires large current fractions and off-axis profiles.

Comparing to the shots #74740 and #49469 with the following predictive current simulations (time intervals in JET 3.0-13.0 s and in JT-60U 5.0-15.0 s), the most important role of the electron density profile was established. This can be noted in a simulation case where the electron density profile in JET was replaced with the profile from JT-60U (#49469 at t = 7.0 s with the largest density gradient at ρ = 0.25-0.5) and in JT-60U with the profile from JET (#74740 at t = 3.0 s). The replaced electron density profiles which have been used in the simulations were constant in time and include the cases with the strongest (in JT-60U) and the smallest (in JET) gradients during the identity shots.

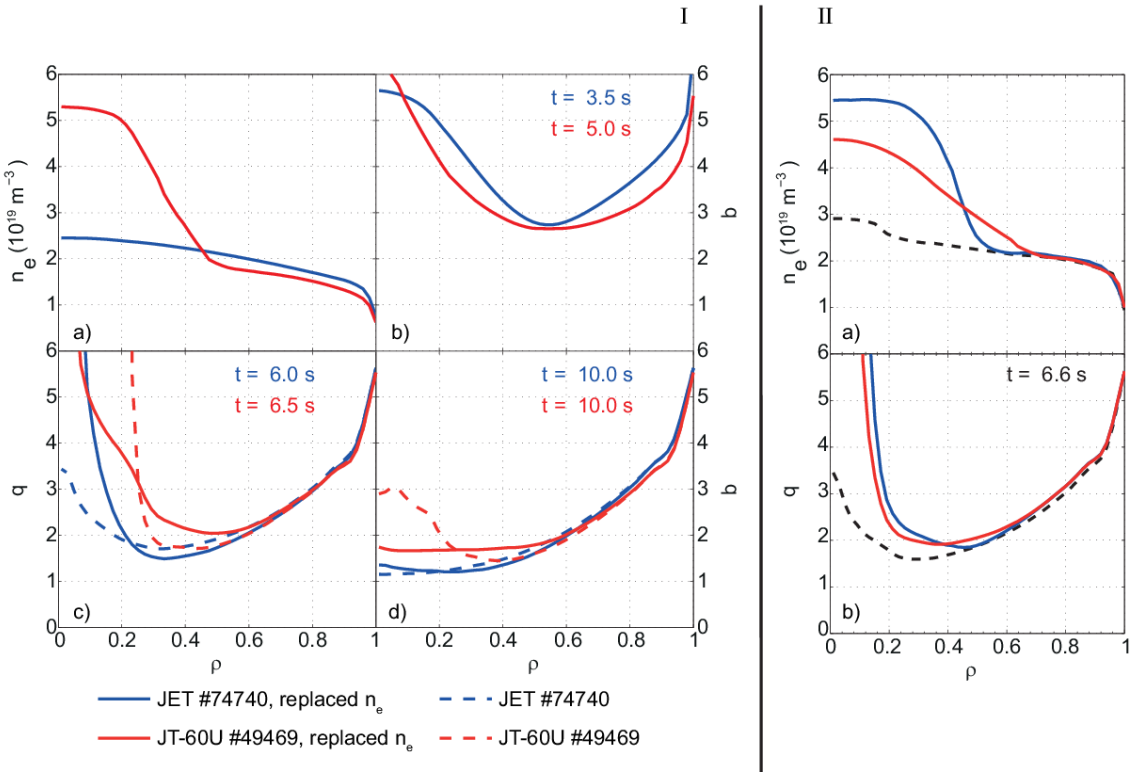

Figure 3: Simulation with the replaced electron density profile: a) Experimental density gradients b) Experimental initial q c)-d) q profile time evolution.
I: Simulation with JET #74740 data (blue dash), JET #74740 data + electron density replaced with the profile JT-60U #49469 (blue solid), simulation with JT-60 #49469 data (red dash), JT-60U #49469 data + electron density replaced with the profile JET #74740 (red solid)
II:Simulation with JET #74740 data with different (non-experimental) density gradients.

Interpretation of the steady-state properties is also done by studying the critical bootstrap current condition [8]. Bootstrap currents and critical bootstrap currents have been presented with the experimental cases in Figure 4. Satisfying of the critical bootstrap condition compared with the experimental cases shows that the same density gradient gives a larger effect on the bootstrap current. The same effect can be noticed also with the testing of the sensitivity of the density gradient (few cases in Figure 3.II.a). The bootstrap fraction in JET with the replaced density profile is smaller by approximately a factor of two than in JT-60U, which means 0.13 MA less bootstrap current in JET. Since the difference in temperature is minor, electron density is the most significant property in increasing the bootstrap current.
The reasons which cause forming of the steep density gradient in JT-60U are not clearly clarified in the previous analysis [2]. The large density ITB has not been observed in JET in this experiments, and on the basis of these simulations, steep density gradients in the beneficial region $0.25 < \rho < 0.6$ would not help to sustain the reverse shape of q for longer than 5-10 seconds and also, adding of external current does not lead to fulfilling of the steady-state condition.

5. CONCLUSIONS

The most important role of electron density gradient in the different time evolution of q is found in these predictive current diffusion simulations. However, the effect of density gradient for the generating bootstrap current density is different in JET and JT-60U. Steady-state prospects have been studied by long 15-20-second simulations and analysing the critical bootstrap current density profiles. The reverse q (with stationarily located

minimum q) is sustained in JT-60U where the bootstrap current is a significant component of the total plasma current. A significant error source in the analysis of the critical bootstrap current density is the rough approximation of the bootstrap current which (together with the lack of quantitative experimental evidence) should be considered when interpreting the critical bootstrap current density profile.
The cause for the electron density peaking which was one of the most significant differences between discharges #74740 and #49469 was not clarified by this analysis. For this, predictive temperature and density simulations are required and will be the focus of further studies in future.

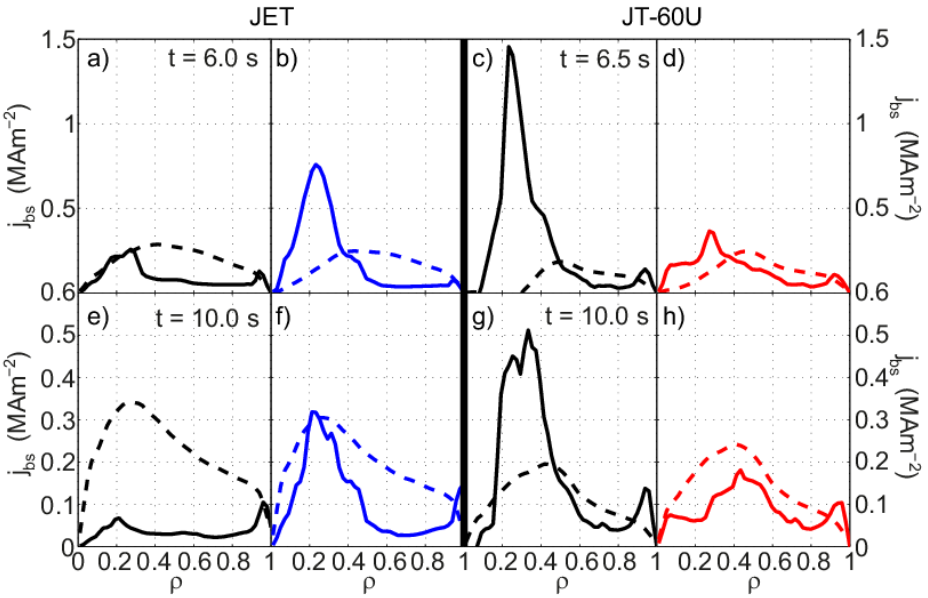

Figure 4: Simulation with the replaced electron density profile: bootstrap current density 49469 (solid: bootstrap current density from NCLASS dash: critical bootstrap current)
a), e) simulation with JET #74740 data
b), f) JET #74740 data + electron density replaced with the profile JT-60U #49469
c), g) simulation with JT-60 #49469 data
d), h) JT-60U #49469 data + electron density replaced with the profile JET #74740.

Acknowledgments
This work was supported by EURATOM and carried out within the framework of the European Fusion Development Agreement. The views and opinions expressed herein do not necessarily reflect those of the European Commission.

This work, supported by the European Communities under the contract of Association between EURATOM- TEKES was partly carried out within the framework of the Task Force on Integrated Tokamak Modelling of the European Fusion Development Agreement.
The views and opinions expressed herein do not necessarily reflect those of the European Commission.

6. REFERENCES

[1] T. S. Taylor et al. 1997 Plasma Phys. Control. Fusion 39 B47
[2] P.C. de Vries et al. 2009 Plasma Phys. Control. Fusion 51 124050
[3] X. Litaudon et al. 2011 Nucl. Fusion 51 073020
[4] G. Genacchi, A. Taroni. Rapporto ENEA RT/TIB/88/5
[5] W. A. Houlberg et al. 1997 Phys. Plasmas 4 3230
[6] J. A. Heikkinen et al. 2001 Journal of Computational Phys. 173 527-548
[7] J. G. Cordey et al. 1988 Plasma Phys. Control. Fusion 30 11 1625-1635
[8] J. Garcia, G. Giruzzi. 2012 Plasma Phys. Control Fusion 54 015009